

INFRARED TECHNIQUES FOR NATURAL CONVECTION INVESTIGATIONS IN CHANNELS BETWEEN TWO VERTICAL, PARALLEL, ISOTHERMAL AND SYMMETRICALLY HEATED PLATES.

Wersja robocza

Witold M. Lewandowski*
Michał Rymś
Hubert Denda

Faculty of Chemistry, Department of Chemical Apparatus and Theory of Machines, Gdansk University of Technology, ul. G. Narutowicza 11/12, 80-233 Gdansk, Poland
*wlew@pg.gda.pl

Keywords

natural convection, infrared imaging, vertical channels, vertical symmetrically heated plates

Abstract

The effect of the gap width between two symmetrically heated vertical, parallel, isothermal plates on intensity of natural convective heat transfer in a gas ($Pr = 0.71$) was experimentally studied using the balance and gradient methods. In the former method heat fluxes were determined based on measurements of the voltage and electric current supplying the heaters placed inside the walls. In the latter, heat fluxes were calculated from the temperature distribution in the air in the plane perpendicular to the surface of the heating plates. Temperature fields were visualised using a thermal imaging camera. The analysis was conducted on two parallel vertical plates of height $H = 0.5$ m and width $B = 0.25$ m with the heated surfaces facing each other. Vertical planes with peripherally open channels and three different distances $s = 0.045, 0.08$ and 0.18 m were created this way. The surface temperature of the heating plates t_w was changed every 5 K and set at $t_w = 30, 35, 40, 45, 50, 55, 60, 65, 70, 75$ and 80 °C, while the ambient temperature range was from 18 to 25 °C.

1. Introduction

Heat transfer by natural convection is not only a theoretically difficult research problem; it is also a tricky one to tackle experimentally. Measurements of temperature, velocity and heat fluxes, are very hard to make owing to their very small and continually changing values in moving convective streams. However, this method of heat transfer is attractive because it is reliable, simple and cost-effective, especially in construction, electronics and power engineering. Natural convection, on the other hand, despite the low intensity of heat exchange due to the large amount of heat transferred from the surfaces of buildings, industrial facilities, power transmission lines, etc., causes gigantic energy losses. An important, but rarely studied research topic relating to naturally occurring convection is heat transfer within a channel formed by two vertical walls. We come across this in heating technology (radiators), buildings and electronics, energetics, household devices, and many other situations.

Natural convection in a vertical plane channel is not an unequivocally defined problem [1], [2], as the following configurations of heat transfer within the channel can occur:

- vertical cavity (by Rayleigh-Bénard convection in a closed space) [3], [4], [5], [6], [7], [49],
- vertical flat gap partially heated [48] or opened (from the bottom, top or from all sides) [8], [9],
- vertical natural convection arrays for the following conditions:
 - asymmetric (hot-cold, hot-adiabatic, warm-hot) isoflux [18], [21], [40], [41], [46], [48] or isothermal heating plates [10], [11], [12], [13], [14], [16], [21], [40], [41], [47], [50], [52], [53], [60]
 - symmetric: isoflux [40], [41], [51] or isothermal heating plates [12], [21], [40], [41], [45],
- vertical plane channel with different wall temperature (hot-cold, hot-adiabatic, warm-hot) [16], [17], [26]
- vertical plane with an open-ended channel and isothermal, symmetrically heated walls [19], [20], [21],

Any of these configurations can be investigated theoretically (analytically: [21], [40], [38], numerically: [7], [11], [14], [19], [20], [24], [26], [27], [28], [32], [35], [36], [37], [48], [50], [52], [53], [58], [59]), experimentally: [7], [8], [12], [16], [18], [20], [29], [30], [31], [35], [39], [52], [53], [60] or tested by visual methods [42], [43], [49].

Within the context of the above division, the current work concerns the experimental and visual study of natural convection heat transfer within a vertical plane channel formed by two vertical, parallel, isothermal, symmetrically heated walls.

The first results of an experimental and theoretical study of natural convective heat transfer in a vertical channel were published in 1942 by Elenbass [21], who carried out investigations on square vertical plates. By analysing a simplified set of equations, and by adjusting constants to fit experimental data, he proposed the following equation for the Nusselt number as a function of the modified Rayleigh number Ra^* , called the Elenbass Rayleigh number:

$$Nu_0 = \frac{Ra^*}{24} \cdot (1 - e^{-35/Ra^*})^{3/4} \quad (1)$$

This equation, confirmed by experimental studies, is valid for the range $10^{-1} < Ra^* < 10^5$ and for fairly short vertical plates in air. In addition, for $10^4 < Ra^* < 10^9$ it has two asymptotes: one for small values of the s/H ratio (fully developed flow regime) and the other for large values of s/H (boundary layer flow regime).

Further studies of natural convection in vertical open channels were published by Raithby and Hollands [22] and [23], and Aung, Fletcher and Sernas [17], who derived a different relation that also captures both limiting cases $s \rightarrow 0$ and $s \rightarrow \infty$. After modifying the relation (1), they obtained a new version of the Elenbass equation:

$$Nu_0 = (Nu_{fd}^m + Nu_{bl}^m)^{1/m}; \quad m = -1.9, \quad (2)$$

where Nu_{bl} is the Nusselt number for the boundary layer regime near the entrance and Nu_{fd} is the Nusselt number for fully developed flow throughout the flow passage along the greater part of the channel.

$$Nu_{bl} = 0.62 \cdot (Ra^*)^{1/4}, \quad \text{for } b \rightarrow \infty \quad (3)$$

$$Nu_{fd} = Ra^*/24, \quad \text{for } b \rightarrow 0, \quad (4)$$

A comparison of equations (1) and (2) with Sparrow and Bahrami's experimental data [8] and Ormiston's numerical solutions [24] is given in [25].

Further research by Churchill and Usagi [45], performed for natural convective heat transfer within a vertical channel with isothermal, symmetrically heated rectangular plates, led to an equation similar to but simpler than (2):

$$Nu_0 = \left[\left(\frac{Ra^*}{24} \right)^{-m} + (0.594 \sqrt[4]{Ra^*})^{-n} \right]^{-1/m}, \quad (5)$$

which is valid for fairly short vertical plates in air and when $10^4 < Ra^* < 10^9$.

From the correlating procedure described by Churchill and Usagi [45], the exponent m in Eq. (5) is equal to approximately 2, so the relationship for the vertical channel with two isothermal, symmetrically heated surfaces takes the form:

$$Nu_0 = \left[\left(\frac{576}{Ra^*} \right)^2 + \frac{2.873}{\sqrt[4]{Ra^*}} \right]^{-1/2}, \quad (6)$$

In turn, Martin, Raithby and Yvanowich [25] focused on short, wide channels $H/b \leq 10$, in which the proportion of fully developed natural convection is larger and interaction with the region below the bottom inlet into the channel cannot be neglected. As a result they proposed a modified version of the relationship between the Nusselt and Rayleigh numbers for the fully developed regime. It can be written thus:

$$\widetilde{Nu}_{fd} = \frac{\widetilde{Ra}}{6} \cdot \left(1 + \sqrt{1 + \frac{12}{\widetilde{Ra}}} \right), \quad (7)$$

with two asymptotes:

$$\widetilde{Nu}_{fd} = \sqrt{\frac{\widetilde{Ra}}{3}} \quad \text{for } \widetilde{Ra} \rightarrow 0, \quad (8)$$

$$\widetilde{Nu}_{fd} = \frac{\widetilde{Ra}}{3} \quad \text{for } \widetilde{Ra} \rightarrow \infty, \quad (9)$$

Eq. (8) represents a new asymptote that accounts for the effect of upstream conditions. Because of the transition to the boundary layer regime, the range of Ra over which the Elenbass asymptote is valid is limited. Eq. (9) is an already known asymptote of the Elenbass equation (1), (4).

In order to span convective heat transfer from the fully developed to the boundary layer regime Martin, Raithby and Yvanowich [25] transformed Eq.3 into:

$$\widetilde{Nu}_{bl} = 0.62 \cdot \widetilde{Ra}^{1/4} \cdot \left(\frac{H}{b} \right)^{3/2} \quad (10)$$

Bar-Cohen and Rohsenow [40] and Bar-Cohen and Schweitzer [41] compared convective heat transfer in a vertical channel between two isothermal, symmetrically heated plates with other configurations, *i.a.* with the specific conditions of isothermal but asymmetrically heated plates and isoflux, and symmetrically and asymmetrically heated ones. No less important, however, is the optimisation of the distance between the heated plates s_{opt} from the intensification point of view for convective heat transfer $Nu_{0,opt}$. Hence, these researchers also provided optimum values of s_{pot} and $Nu_{0,opt}$ for each configuration of two vertical plates (symmetric, asymmetric, isothermal, isoflux) they examined.

For the case considered in this paper (two isothermal, symmetric, vertical plates), expecting heat transfer maximisation, they give the following optimal relations:

$$s_{opt} = 2.714 P^{0.25} \quad \text{and} \quad Nu_{0,opt} = 1.31, \quad (11)$$

The optimum values of the Rayleigh and Nusselt numbers, calculated for the channel from (11), are 54.3 and 1.31 respectively, [40], which exceeds the Elenbass optimum spacing by only 4 % [21].

Another research direction of convective heat transfer within a vertical channel between two parallel vertical plates leads to the analysis of the mechanisms of this phenomenon. These studies can be performed either by determining the values of the temperature and velocity fields in the channel numerically, or through their visualisation. With the values of these fields to hand it is then possible to determine the local heat transfer coefficients and their distribution to heat transfer surfaces.

The numerical modelling of convective structures was carried out by Baïri et al. [7], Herwig using DNS (direct numerical simulation) [10], Zoubir et al. [20], Salih [26] and many others [1], [2].

Visualisation research of this problem was carried out by Wright et al. [42]: they used smoke and interferometry technique images to visualise convective flow patterns within channels.

In turn, Guo, Song, Zhao attempted to investigate these structures using laser speckle photography [43]. Ambrosini, Paoletti and Tanda studied local heat transfer coefficients and isotherm patterns using Schlieren and holographic interferometry. The flow patterns in an asymmetrically heated vertical channel were shown by both flow visualisation techniques based on laser tomography and velocity field measurements in the plane of symmetry of the channel using the 2D - PIV (Particle Image Velocimetry) technique of Polidori et al. [55]. A laser Doppler velocimeter LDV and thermocouples were used by Kato et al. to determine velocity and temperature fields within the channels of electronic devices [44]. Those methods allows to obtain mainly qualitative results, like convective flow patterns determinations,

separation of convective stream or its transformation into free bouiant chimney [42]. The other groups of methods are focused on studies which gives aspecially quantitative information about particular convection heat transfer problems [44], [55].

Above mentioned methods of temperature and velocity fields indication in natural convective heat transfer phenomenons however usually needs expensive devices and time consuming procedures. Alternatively to both method groups the infrared imaging method can be proposed. It was previously introduced and tested with promising results [57] and can be to used for quantitative and qualitative studies as well.

The aim of the present work is to investigate convective heat transfer within a channel consisting of two parallel, vertical plates at three given spacings **base of thermal infrared imaging method**. These isothermal plates were heated symmetrically with ten different power heating settings. Local heat transfer coefficients and isotherm patterns were recovered by **the procedure from** [57]. Once the results have been found consistent with those of other researchers, they will offer a better understanding of the scientifically and technically very important issue of heat transfer in channels.

This study should allows to obtain the distributions of local heat transfer coefficients on isothermal vertical walls creating opam channels with different distances between heated surfaces s as well as the convective flow patterns between them.

The experiments were carried out at the Department of Chemical Apparatus and Theory of Machines, Faculty of Chemistry, Gdańsk University of Technology, and the results compared with those stated above.

2. Methodology

2.1. Testing device

The testing device used in this investigation is shown in Fig.1. It consists of two identical vertical plates, symmetrically heated to a constant isothermal temperature of both surfaces. Each plate is constructed from three aluminium sheets of height 0.495 m and width 0.247 m but with different thicknesses (0.012 m external, 0.010 m central and 0.010 m internal). Two flat heaters are placed inside each plate according to scheme in Fig.2. The main heater (300 W) is sandwiched between the external aluminium sheet, a 0.006 m thick rezotex layer and the central sheets. The second, auxiliary heater (150 W) is placed between the internal aluminium sheet and the bottom rezotex layer (0.006 m).

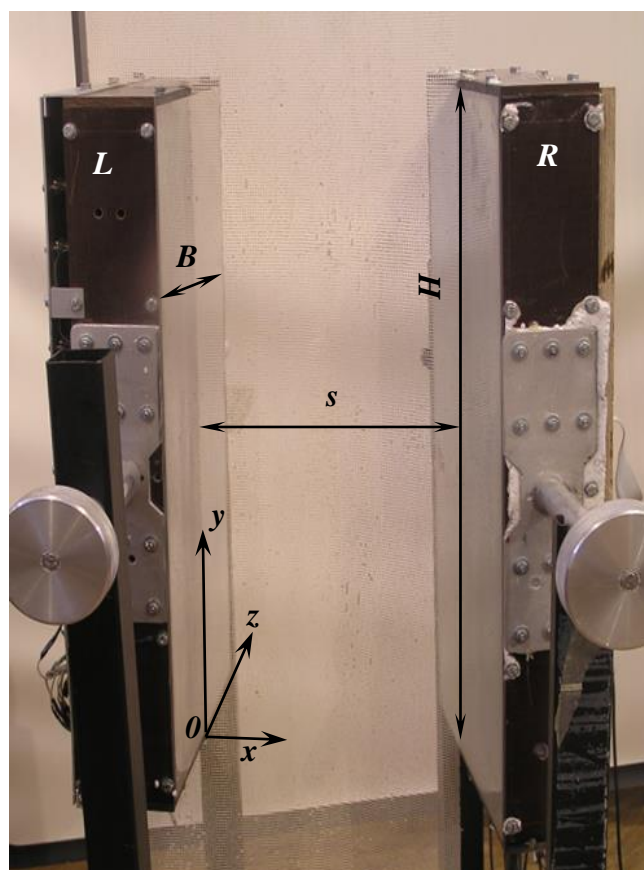


Fig.1 The experimental device consisting of two perpendicular panels and a grid placed across the gap between them.

A cross-section of one of the two identical vertical heating plates used in this study is shown in Fig.2.

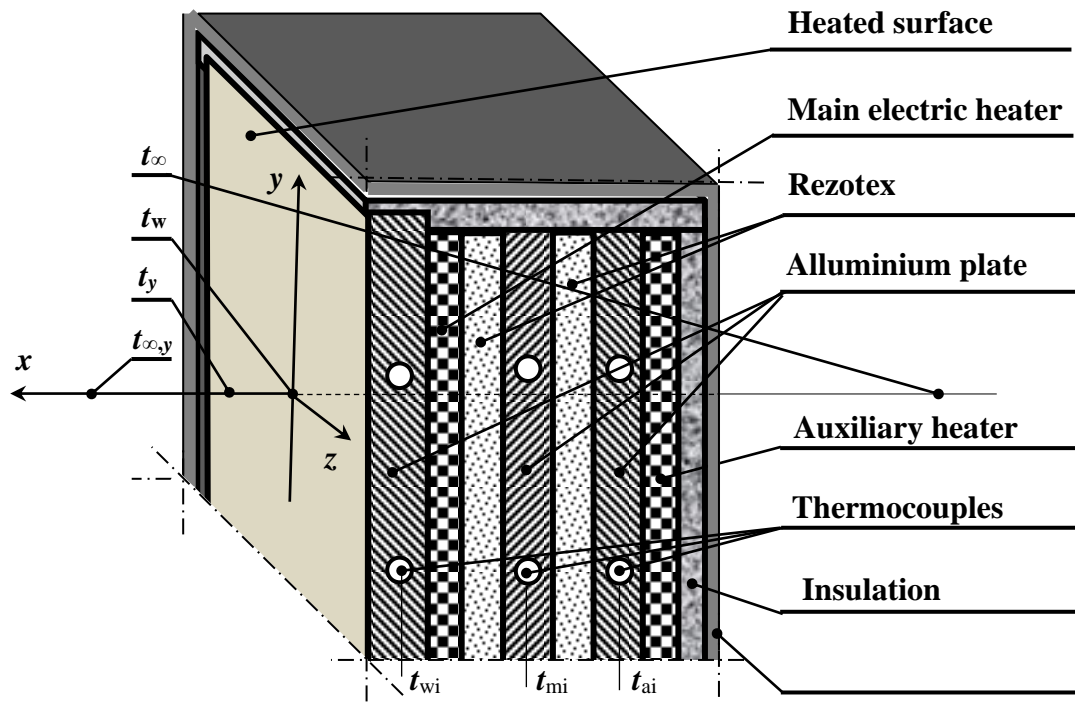


Fig.2 Cross-section of the upper left corner of the left-hand heated vertical plate from Fig.1.

On each experimental plate the values indicated by the thermocouples were taken to be the following temperatures: of the surface of the vertical heating plates t_w (average of 4 thermocouples placed within the external aluminium panels), of the surface of the rezotex plate on the side of the main heater t_m (4 thermocouples), and of the side of auxiliary one t_a (4 thermocouples). 32 thermocouples were used in the experimental device: 12 in one and another 12 in the second vertical heating plate, with the remaining 8 being distributed throughout the surrounding area undisturbed by heat transfer.

The regulation system automatically maintains the pre-set temperature of the heating surface t_w by adjusting the power of the main heater $N = U \cdot I$ and simultaneously that of the auxiliary heater, so that the temperature difference on both sides of the rezotex partition remains equal to zero $\Delta t = t_m - t_a = 0$. With $\Delta t = 0$ and narrow plates it can be assumed that the whole heater power from both heated surfaces will be transformed into a heat flux $Q = N_1 + N_2 = U_1 \cdot I_1 + U_2 \cdot I_2$, and then transferred by convection to the air inside the channel between the two vertical plates. The aluminium outer surfaces of both plates were polished in order to minimise heat transfer by radiation.

One of these plates, previously used to test the new method of measuring heat fluxes in air using a thermal imager, is described in detail in [57]. In the present study we use the same method of measuring the heat flux using a thermal imaging camera; hence, the theoretical basis and test procedures of this method are also given in [57].

Consequently, the method of measuring convective heat flows and heat transfer based on the visualisation of temperature fields of convective flow patterns in air using a thermal imaging camera in this work is described only briefly. Instead, we focus on the results that were obtained using it.

2.2. Description of the measurement method

Since air within the range of natural convection temperatures (0 - 100 °C) does not emit radiation in the mid-infrared (wavelengths from approx. 1 to 15 μm) range of the camera's sensitivity, a plastic mesh was used in order to detect this radiation. The grid, placed parallel to the flow of the convective heat flux and perpendicular to the heating surface, has the temperature of the surrounding air. The heated mesh filaments are already visible to the IR camera. The low coefficient of thermal conductivity and the small diameter of the fibres prevents the equalisation of the temperature on the mesh surface. **The frequency of convective stream fluctuations in the air is much greater than thermal inertia of the mesh, therefore detected temperature is averaging in the time. It is close to stationary conditions, assumed in our consideration.**

The results of preliminary tests of different grids cooperating with the IR-FlexCam® Fluke Ti35 enabled the most suitable one to be selected for visualising the temperature fields in the vertical gaps during convective heat transfer. The chosen grid had the following parameters: cotton impregnated with polyester material, with a thermal conductivity $\lambda = 0.02 \text{ W/(m}\cdot\text{K)}$, mesh size $a = 1.6 \text{ mm}$, and fibre diameter $d = 0.4 \text{ mm}$.

Stretched over the frame (Fig.1) and stiffened with polyester lacquer spray, the mesh was placed perpendicular to the heating surfaces. A grid was cut out for each slot width $s = 0.045, 0.08$ and 0.18 m and placed perpendicular to the plates at their half-width $z = B/2$.

The analysis was performed using two vertical plates of height $H = 0.5 \text{ m}$ and a width $B = 0.25 \text{ m}$ with the heating surfaces arranged in parallel and close to each other. Vertical planes with peripherally open channels and three different spacings $s = 0.045, 0.08$ and 0.18 m were created this way.

The surface temperature of the heating plates t_w was changed at 5 K intervals: $t_w = 30, 35, 40, 45, 50, 55, 60, 65, 70, 75$ and $80 \text{ }^\circ\text{C}$, while the ambient temperature ranged from 18 to 25 °C. The temperature field in the channel, in the plane perpendicular to the heated surfaces, located exactly between the plates $z = B/2$, was identified with the IR camera and the grid as air radiation detector. This decision was taken as a result of previous studies which had shown that the z coordinate had no significant impact on the results. The temperature fields in the three cross-sections of the boundary layer $z = 0.0, z = 0.25 B$ and $z = 0.5 B$ are qualitatively convergent [57].

All the tests described in this paper were conducted using a FlexCam® Fluke Ti35 IR camera with a resolution specified by the manufacturer as $\leq 0.1 \text{ K}$ in the temperature range - 20 - 100°C. It was set up at a constant distance of 2 m from and perpendicular to the grid and parallel to the heating surfaces.

3. Results and discussion

3. 1. Results of temperature field and temperature gradient investigations

The results of the temperature field visualisation within the cross-sectional plane inside the gaps between the two vertical isothermal left- (L) and right-hand (R) plates obtained using an IR camera are shown in Fig. 3 for $s = 0.045 \text{ m}$, Fig. 4 for $s = 0.085 \text{ m}$ and Fig. 5 for $s = 0.18 \text{ m}$.

For technical reasons, it is impossible to illustrate graphically on one photograph the temperature distribution of the heating surface and the temperature field on the mesh: when the IR camera's sensitivity is focused on higher plate temperatures, the temperature field on the mesh lies beyond the temperature scale and vice versa. Therefore, when the temperature fields of the air are visualised, the surface temperature of the plate, which is beyond the temperature scale, is shown in grey. However, this has no effect on the results of the

calculations, since these are carried out with the temperature field data digitally stored by the IR camera.

The digital values of temperature distributions on the $(x, y, z=B/2)$ plane, perpendicular to the two vertical heating walls at both ends of the channel, are presented graphically in Fig. 3 - 5 and also listed in Table 1.

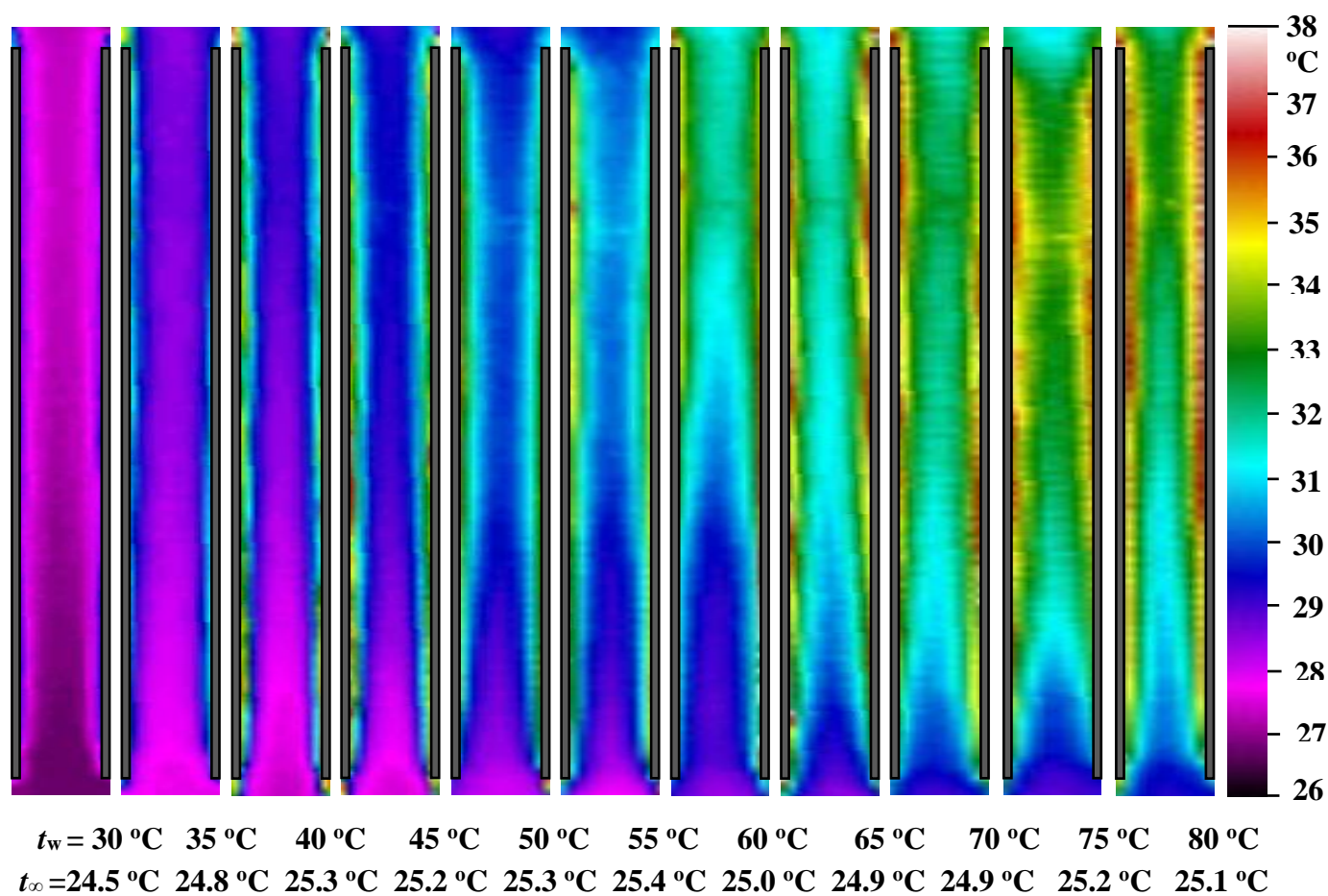


Fig.3 Temperature fields in the gap $s = 0.045$ m between the vertical isothermal heated plates as a function of their surface temperature t_w and the ambient temperature t_∞ in the $x, y, z=B/2$ planes.

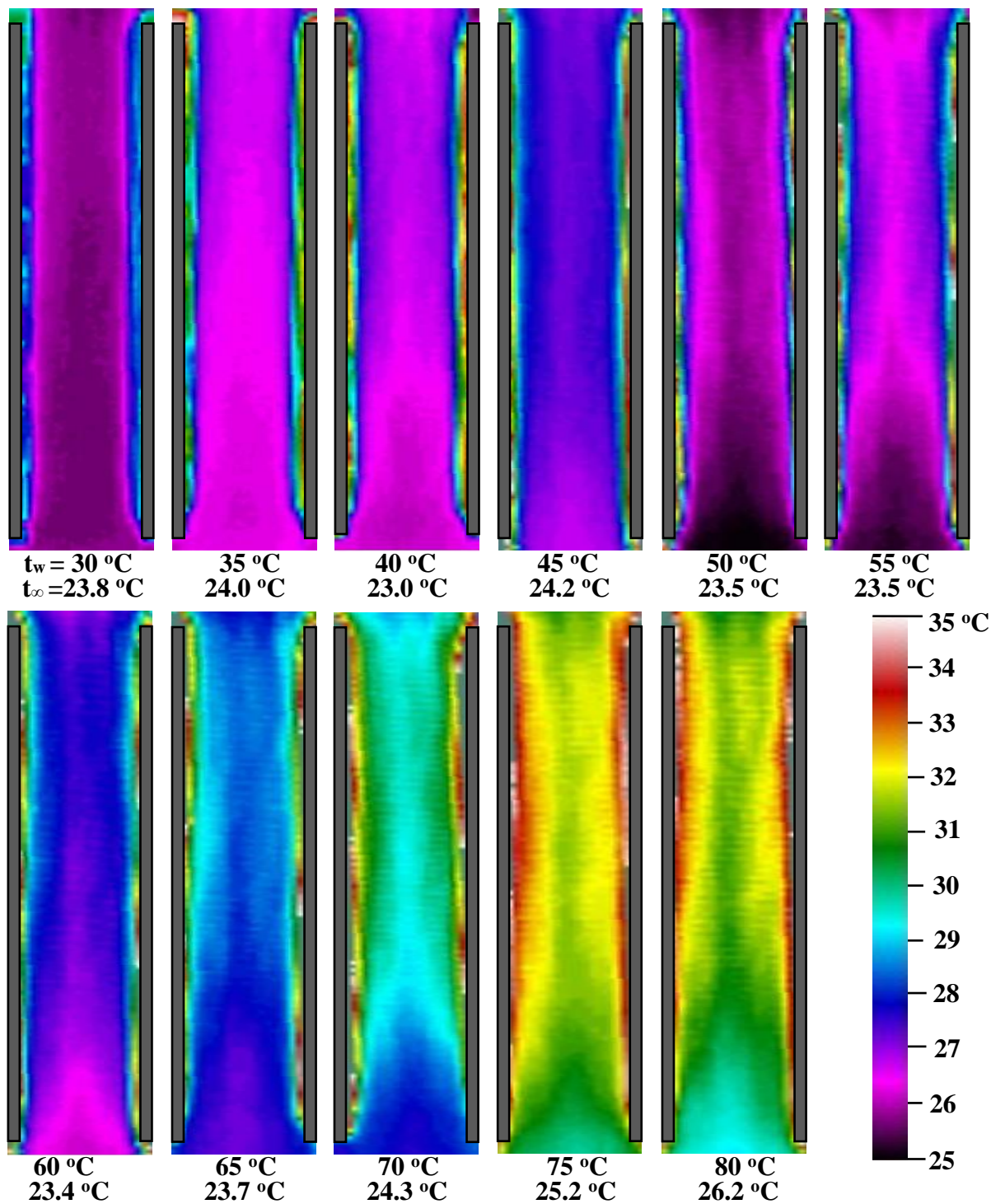


Fig.4 Temperature fields in the gap $s = 0.085$ m between the vertical isothermal heated plates as a function of their surface temperature t_w and the ambient temperature t_∞ in the $x, y, z=B/2$ planes..

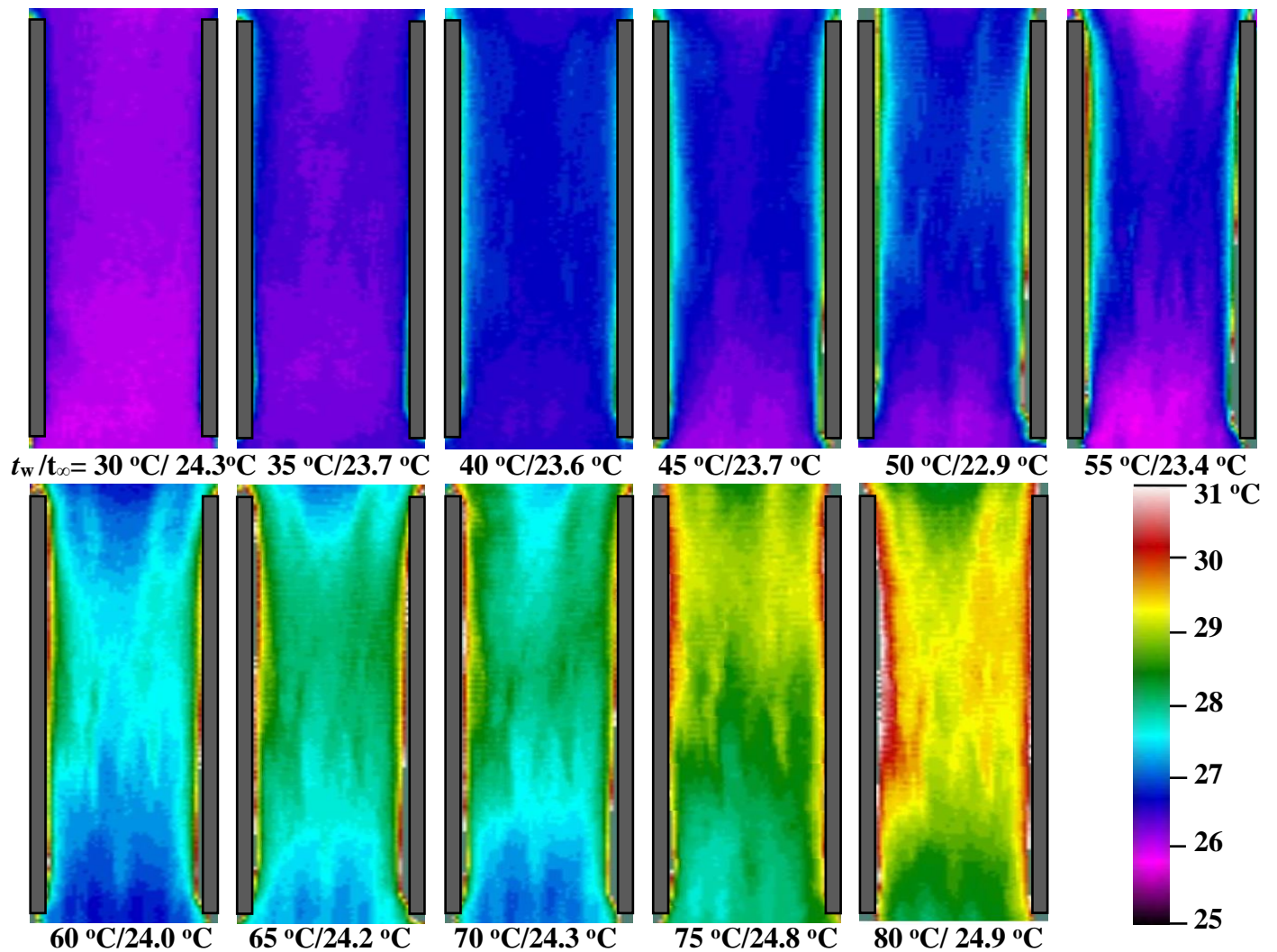


Fig.5 Temperature fields in the gap $s = 0.18$ m between the vertical isothermal heated plates as a function of their surface temperature t_w and the ambient temperature t_∞ in the $x, y, z=B/2$ planes.

Some examples of these distributions inside the three channels ($s = 0.045, 0.85$ and 0.18 m) in the $(x, y, z = B/2)$ plane at the leading edges $y = 0$, at mid-height $y = H/2$ and at the trailing edges $y = H$ of the channels are shown in Fig.6.

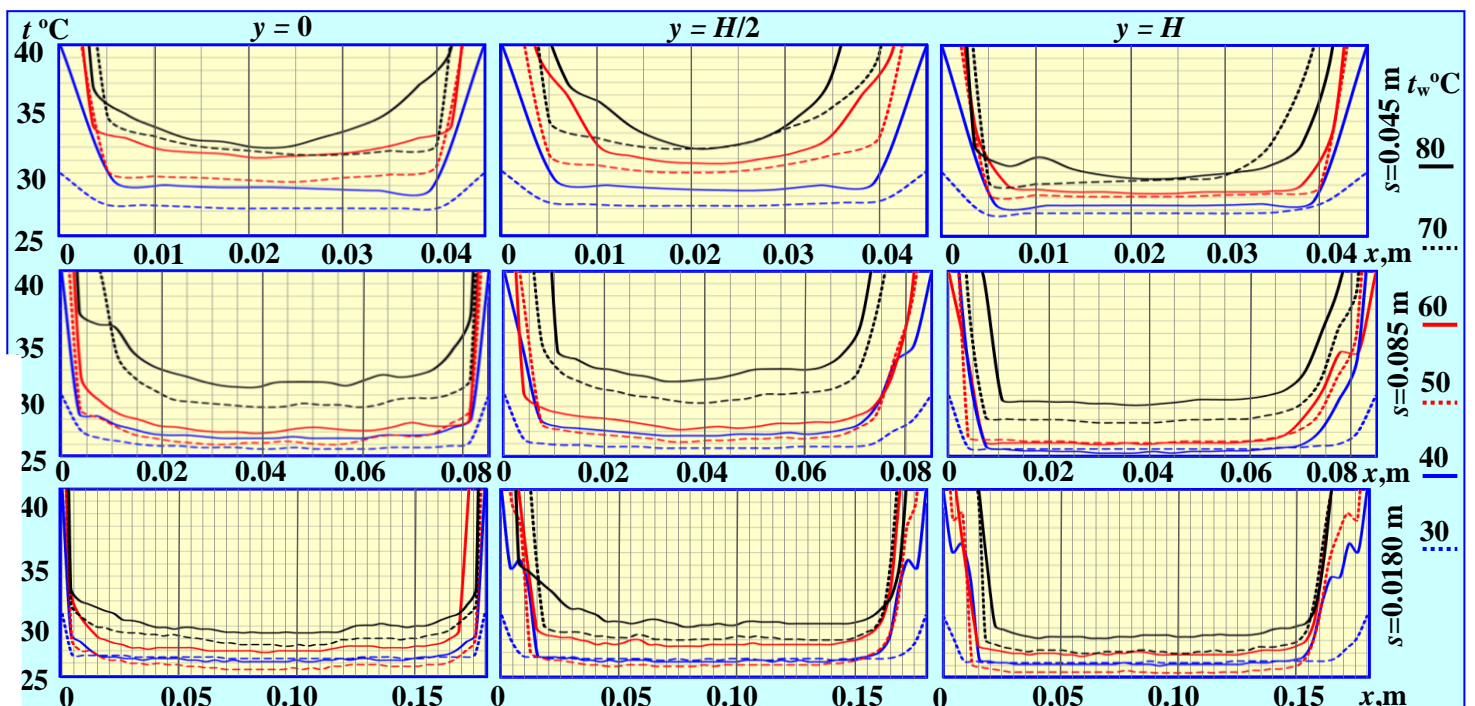


Fig.6 Temperature distribution across three gaps ($s = 0.045, 0.85$, and 0.18 m) in the x -axis perpendicular to the heated plates, as a function of their surface temperature ($t_w = 30, 40, 50, 60, 70$ and 80 °C) measured on three specific levels $y = 0$ (leading edge), $H/2$ and H (trailing edge).

In this figure the temperature range has been limited to 40 °C for better clarity. The temperature variations in the channels along the lines perpendicular to the heating surfaces x , over a wider range of temperature variation from 25 to 80 °C, but only at level $y = H/2$ for set temperatures of the heated vertical plates $t_w = 30, 40, 50, 60, 70$ and 80 °C are shown in Figure 7.

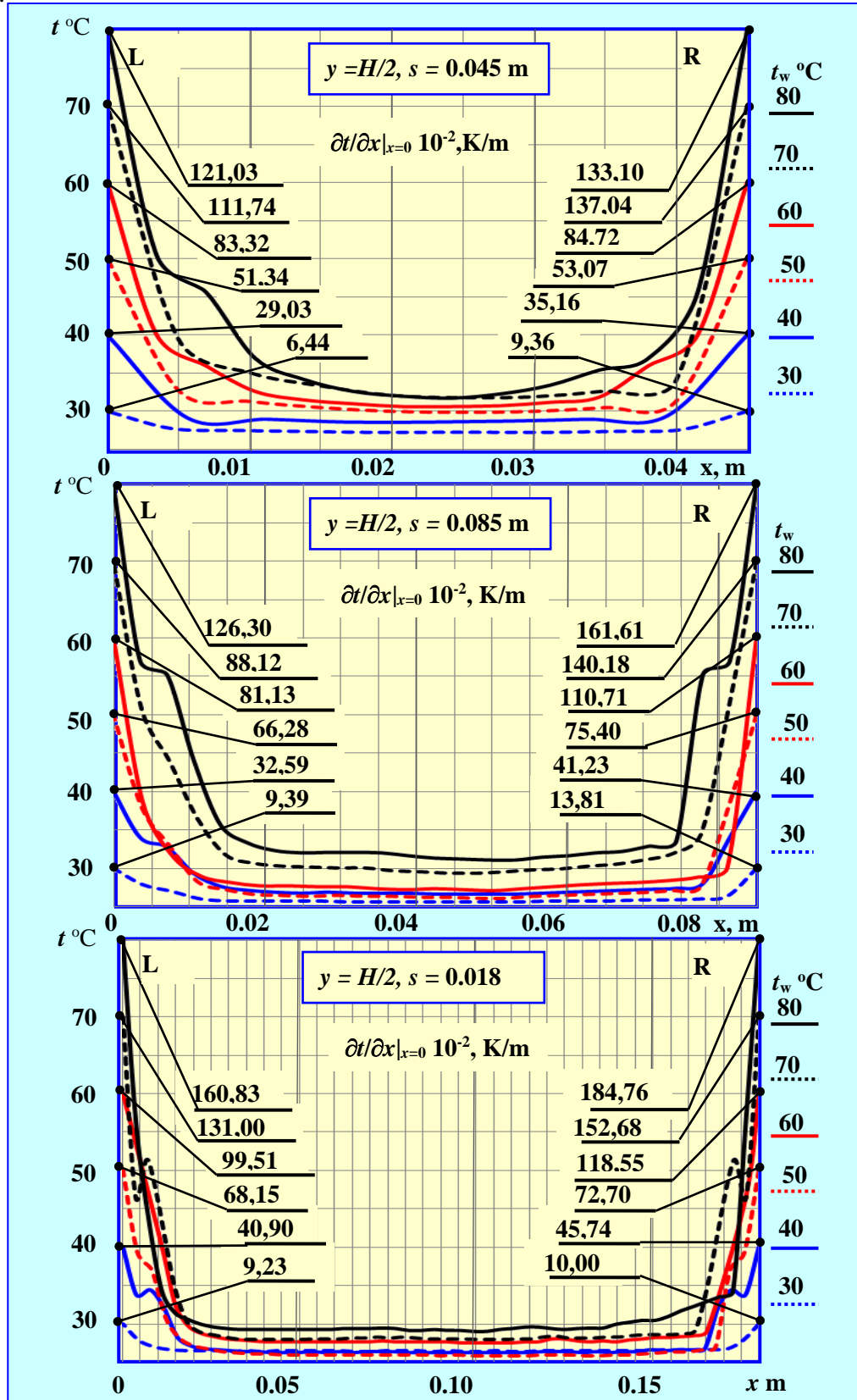


Fig.7 Temperature and temperature gradient distributions perpendicular to two vertical parallel heated surfaces that form three channels with spacings $s = 0.045, 0.85$, and 0.18 m, measured at $y =$

$H/2$ and $z = B/2$, as a function of the temperature $t_w = 30, 40, 50, 60, 70$ and 80 °C of the heated surfaces.

In addition to the temperature distributions Fig. 7 also shows the calculated values of the temperature gradients $dt/dx|_{x=0}$ on both heating surfaces (L) and (R) at points $y = H/2$ and $z = B/2$.

From the digital data generated, apart from the photos, by the IR camera and partially listed in Table 1, the temperature gradients $dt/dx|_{x=0}$ and their distributions on the left- and right-hand heated walls of the vertical channels were calculated on the basis of equation (12):

$$\left. \frac{\partial t}{\partial x} \right|_{x=0,L} = \frac{(t_0=t_w)-t_1}{x_1-(x_0=0)} \quad (\text{L}) \quad \text{and} \quad \left. \frac{\partial t}{\partial x} \right|_{x=0,R} = \frac{(t_n=t_w)-t_{n-1}}{(x_n=s)-x_{n-1}} \quad (\text{R}). \quad (12)$$

The results of the numerical calculations, independently for the left- (L) and right-hand (R) heated walls, for the four channels ($s = 0.045; 0.085$ and 0.18 m) in the form of temperature gradients $dt/dx|_{x=0,y}$ for wall temperatures from $t_w = 30$ to 80 °C at 5 K intervals at different heights of the channel ranging from $y=0$ (leading edges of the channels) to $y = H$ (trailing edges of the channels) for $z = B/2 = \text{constant}$ are listed in Tables 2, 3 and 4.

Table 2. Temperature gradient distributions along the left- and right-hand (separated by a slash) vertical plates of constant surface temperature $t_w = 30, 35, 40, 45, 50, 55, 60, 65, 70, 75$ and 80 °C within a channel of width between the heated plates $s = 0.045$ m.

	$\partial t / \partial x _{x=0,y} \text{ (L)} / \partial t / \partial x _{x=0,y} \text{ (R)}, \quad \text{K/m}$										
$t_w, ^\circ\text{C}$	30	35	40	45	50	55	60	65	70	75	80
$t_w, ^\circ\text{C}$	24.5	24.8	25.3	25.2	25.3	25.4	25	24.9	24.9	25.2	25.1
y, m	644/	1630/	2868/	4222/	5765/	6722/	8332/	10252/	11816/	10728/	12630/
0.0	982	2506	3574	4940	5608	7253	8530	12262	14119	14000	13929
0.035	543/	1407/	2648/	3796/	5524/	6586/	8000/	9851/	11273/	9946/	12171/
	936	2485	3536	4902	5395	7143	8357	12173	13959	13980	1331
0.070	543/	1443/	2716/	3921/	5393/	6551/	8036/	9890/	11174/	9981/	12138/
	936	2485	3436	4821	5341	7051	8339	12151	13889	13790	13214
0.105	527/	1481/	2648/	3796/	5339/	6519/	7908/	9931/	11174/	9846/	11934/
	936	2485	3516	4860	5216	7086	8298	12105	13796	13707	13310
0.140	576/	1517/	2749/	3887/	5301/	6551/	8036/	10069/	11174/	9998/	11899/
	936	2438	3475	4741	5270	6920	8298	12062	13748	13647	13291
0.175	611/	1556/	2817/	3850/	5301/	6654/	8148/	10031/	11235/	9998/	11983/
	936	2438	3475	4741	5307	6845	8357	12062	13704	13603	13291
0.210	611/	1443/	2852/	3887/	5134/	6551/	8110/	9989/	11215/	10185/	11899/
	936	2485	3516	4699	5253	6827	8394	12062	13796	13603	13291
0.245	644/	1591/	2903/	4009/	5134/	6586/	8332/	10130/	11174/	10354/	12103/
	936	2438	3516	4699	5307	6827	8472	12062	13704	13603	13310
0.280	712/	1630/	2988/	4117/	5095/	6654/	8462/	10211/	11315/	10625/	12255/
	982	2485	3536	4619	5341	6881	8512	12062	13748	13647	13424
31.5	712/	1630/	3056/	4188/	5042/	6722/	8628/	10252/	11414/	10813/	12086/
	982	2485	3536	4661	5429	6955	8648	12062	13889	13647	13483
0.350	780/	1630/	3123/	4330/	5134/	6790/	8815/	10310/	11636/	11016/	12222/
	1025	2485	3574	4699	5537	7086	8840	11994	13796	13750	14006
0.385	780/	1647/	3175/	4418/	5170/	6858/	8924/	10352/	11674/	11272/	12222/
	1025	2485	3616	4661	5679	7143	8840	12015	13796	13853	13870
0.420	815/	1647/	3243/	4577/	4929/	6942/	8963/	10310/	11636/	11560/	12222/
	1071	2485	3655	4481	5838	7143	8744	12015	13704	13937	13833
0.455	847/	1686/	3327/	4702/	5060/	7045/	9037/	10390/	11716/	11899/	12526/
	1071	2485	3696	4500	5963	7143	8821	12015	13841	14040	14102
0.490	883/	1778/	3395/	4932/	6027/	7198/	9295/	10451/	11716/	12374/	13257/
	1114	2485	3857	5143	6159	7979	9536	11947	13748	14563	15148
Average	682/	1581/	2967/	4176/	529/	6729/	8468/	10161/	11423/	10706/	12237/
L/ R	987	2477	3568	4745	5510	7086	8599	12070	13816	13825	13654
Channel	835	2029	3268	4461	5400	6908	8534	11116	12620	12266	12946

Table 3. Temperature gradient distributions along the left- and right-hand vertical plates of constant surface temperature $t_w = 30, 35, 40, 45, 50, 55, 60, 65, 70, 75$ and 80 °C within a channel of width between the plates $s = 0.085$ m.

	$\partial t / \partial x \big _{x=0,y} \text{ (L)} / \partial t / \partial x \big _{x=s,y} \text{ (R)}, \text{ K/m}$										
$t_w, ^\circ\text{C}$	30	35	40	45	50	55	60	65	70	75	80
$t_{cs}, ^\circ\text{C}$	23.8	24	23	24.2	23.5	23.5	23.4	23.7	24.3	25.2	26.2
y, m	744/ 1422	1934/ 2848	3175/ 4373	4261/ 6293	6462/ 7707	6978/ 9207	7741/ 11471	9512/ 12429	7314/ 14329	10580/ 13661	12086/ 16551
0.0											
0.035	648/ 1381	1510/ 2803	2613/ 4250	3599/ 6161	6222/ 7500	6111/ 8980	5872/ 11271	7863/ 12363	5926/ 14150	10142/ 13500	1134/ 16420
0.070	713/ 1381	1698/ 2803	2852/ 4207	3802/ 6161	6258/ 7417	6315/ 8897	6434/ 11250	8377/ 12322	6652/ 14150	10096/ 13619	11543/ 16354
0.105	809/ 1381	1817/ 2762	2988/ 4123	3971/ 6071	6332/ 7373	6687/ 8897	7062/ 11114	8908/ 12170	7407/ 13971	10207/ 13481	11815/ 16205
0.140	843/ 1381	1901/ 2762	3088/ 4083	4039/ 6050	6332/ 7373	6823/ 8790	7317/ 11114	9032/ 12125	7716/ 13971	10321/ 13481	12103/ 15967
0.175	874/ 1381	1969/ 2762	3140/ 4123	4074/ 6114	6427/ 7500	6978/ 8750	7553/ 11204	9316/ 12256	8025/ 14018	10466/ 13481	12323/ 16009
0.210	907/ 1422	2070/ 2803	3208/ 4123	4175/ 6114	6519/ 7540	7130/ 8833	7792/ 11250	9688/ 12256	8519/ 14107	10614/ 13539	12494/ 16074
0.245	939/ 1381	2138/ 2717	3259/ 4123	4226/ 6050	6628/ 7540	7282/ 8603	8113/ 11071	9867/ 12256	8812/ 14018	10630/ 13439	12630/ 16161
0.280	1003/ 1336	2205/ 2717	3327/ 4083	4329/ 5961	6702/ 7583	7401/ 8373	8368/ 10961	10043/ 11911	9136/ 13861	10809/ 13400	12749/ 15967
31.5	1037/ 1295	2241/ 2676	3395/ 4123	4414/ 5961	6776/ 7623	7502/ 8123	8556/ 10804	10134/ 11780	9368/ 13907	10889/ 13400	12901/ 15967
0.350	1037/ 1250	2241/ 2589	3463/ 4000	4378/ 5961	6815/ 7623	7605/ 7750	8520/ 10536	10222/ 11565	9444/ 13771	10920/ 13359	12953/ 16009
0.385	1068/ 1208	2273/ 2458	3531/ 3897	4481/ 5961	6924/ 7707	7741/ 7500	8675/ 10289	10364/ 11220	9659/ 13771	11019/ 13259	13105/ 16009
0.420	1037/ 1163	2309/ 2310	3563/ 3707	4566/ 6004	6999/ 7790	7841/ 7083	8724/ 10000	10452/ 10789	9906/ 13907	11179/ 13118	13309/ 15881
0.455	1068/ 1208	2341/ 2310	3599/ 3563	4650/ 6004	7037/ 7833	7877/ 7270	8827/ 9643	10506/ 10595	10109/ 13929	11358/ 13079	13545/ 15922
0.490	1102/ 1422	2377/ 2803	3735/ 4000	4786/ 6204	7147/ 8040	8012/ 8937	9063/ 10246	10611/ 11479	10323/ 14621	11537/ 13940	13681/ 17089
Average L/R	922/ 1334	2068/ 2675	3262/ 4052	425/ 6071	6639/ 761	7219/ 8400	7908/ 10815	966/ 11834	8554/ 14032	10718/ 13450	12572/ 16172
Channel	1128	2372	3657	5161	7125	7810	9362	10747	11293	12084	14372

Table 4. Temperature gradient distributions along the left- and right-hand vertical plates of constant surface temperature $t_w = 30, 35, 40, 45, 50, 55, 60, 65, 70, 75$ and 80 °C within a channel of width between the plates $s = 0.180$ m.

	$\partial t / \partial x \big _{x=0,y} \text{ (L)} / \partial t / \partial x \big _{x=s,y} \text{ (R)}, \text{ K/m}$										
$t_w, ^\circ\text{C}$	30	35	40	45	50	55	60	65	70	75	80
$t_{cs}, ^\circ\text{C}$	24.3	23.7	23.6	23.7	22.9	23.4	24	24.2	24.3	24.8	24.9
y, m	957/ 1167	3049/ 3414	4127/ 4661	5864/ 6107	6815/ 7957	9026/ 10998	10211/ 12381	11716/ 14141	13199/ 15386	13253/ 18170	16667/ 19093
0.0											
0.035	886/ 1083	2969/ 3393	4049/ 4574	5710/ 6027	6702/ 7833	8705/ 10808	10069/ 12236	11495/ 14023	13000/ 15338	12596/ 18071	16187/ 18998
0.070	886/ 1083	2969/ 3393	4049/ 4574	5670/ 5985	6667/ 7707	8647/ 10571	9931/ 12023	11235/ 13855	13019/ 15315	12559/ 17997	16000/ 18857
0.105	886/ 1040	2969/ 3393	4049/ 4530	5633/ 5905	6667/ 7540	8606/ 10427	9851/ 11950	11273/ 13760	13019/ 15268	12596/ 17875	15937/ 18857
0.140	886/ 1040	3008/ 3393	4049/ 4574	5633/ 5905	6741/ 7457	8705/ 10381	9890/ 11905	11235/ 13691	13019/ 15268	12691/ 17824	15937/ 18712
0.175	886/ 1000	3008/ 3393	4049/ 4574	5593/ 5905	6741/ 7417	8747/ 10213	9890/ 11950	11273/ 13642	12920/ 15268	12827/ 17824	15937/ 18712

0.210	923/ 1040	3008/ 3393	4049/ 4574	5593/ 5866	6776/ 7333	8785/ 10000	9951/ 11950	11353/ 13691	13019/ 15315	13000/ 17899	15980/ 18594
0.245	923/ 1000	3049/ 3393	4090/ 4574	5556/ 5905	6815/ 7270	8785/ 9714	9951/ 11855	11353/ 13596	13100/ 15268	13272/ 17899	16083/ 18476
0.280	923/ 1000	3049/ 3304	4049/ 4574	5593/ 5905	6815/ 7167	8827/ 9333	10069/ 11787	11456/ 13596	13141/ 15268	13272/ 17875	16167/ 18118
31.5	923/ 873	3049/ 3257	4090/ 4530	5633/ 5866	6889/ 6937	8866/ 8739	1013/ 11855	11536/ 13642	13160/ 15223	13426/ 17899	16270/ 17787
0.350	923/ 873	3049/ 3168	4090/ 4488	5633/ 5744	6924/ 6623	8946/ 8309	10211/ 11737	11536/ 13547	13199/ 15223	13562/ 17580	16333/ 17120
0.385	886/ 833	3049/ 3036	4090/ 4357	5710/ 5625	6963/ 6187	9068/ 7810	10252/ 11619	11594/ 13379	13279/ 15109	13580/ 17164	16500/ 15928
0.420	957/ 750	2969/ 2946	4127/ 4271	5670/ 5545	6963/ 5520	9106/ 7284	10252/ 11429	11536/ 13284	13199/ 15061	13426/ 16598	16583/ 14739
0.455	957/ 647	2927/ 2811	4127/ 4143	5633/ 5464	6924/ 5270	9106/ 7048	10172/ 11238	11495/ 13048	13061/ 14898	12769/ 15593	16373/ 13882
0.490	1028/ 1123	3049/ 3036	4167/ 4315	5941/ 6027	7073/ 7667	9389/ 9570	10390/ 11737	11816/ 13379	13462/ 15268	14003/ 16940	16937/ 16690
Average L/ R	922/ 970	3012/ 3248	4083/ 4488	5671/ 5852	6832/ 7059	8888/ 9414	10081/ 11844	1146/ 13618	1312/ 15232	13122/ 17547	16259/ 17638
Channel	946	3130	4286	5762	6946	9151	10963	12539	14176	15335	16949

3.2. Results of the balance method for measuring convective heat transfer within the channels

The results of studies carried out using the balance method in accordance with the procedure described in [57] for the left- and right-hand heated plates of the channels for different distances s can be written as:

$$Nu_b = 0.489 \cdot Ra_b^{1/4} \text{ (L)}, = 0.492 \cdot Ra_b^{1/4} \text{ (R)}, = 0.491 \cdot Ra_b^{1/4} \text{ (total)}, s = 0.045 \text{ m}, \quad (17)$$

$$Nu_b = 0.477 \cdot Ra_b^{1/4} \text{ (L)}, = 0.482 \cdot Ra_b^{1/4} \text{ (R)}, = 0.480 \cdot Ra_b^{1/4} \text{ (total)}, s = 0.085 \text{ m}, \quad (18)$$

$$Nu_b = 0.482 \cdot Ra_b^{1/4} \text{ (L)}, = 0.511 \cdot Ra_b^{1/4} \text{ (R)}, = 0.497 \cdot Ra_b^{1/4} \text{ (total)}, s = 0.180 \text{ m}, \quad (19)$$

$$Nu_b = 0.461 \cdot Ra_b^{1/4} \text{ (L)}, = 0.510 \cdot Ra_b^{1/4} \text{ (R)}, = 0.486 \cdot Ra_b^{1/4} \text{ (total)}, s = \infty. \quad (20)$$

The left-hand vertical plate (L) was already used in our previous study of convective heat transfer, and the result was published in [57] as:

$$Nu_b = 0.494 \cdot Ra_b^{1/4}. \quad (21)$$

The physical properties in Nusselt and Rayleigh numbers λ , β , α and ν are calculated according to average temperature of air $t_{av} = (t_w + t_{\infty})/2$.

The divergence error between equation (20), currently obtained for the two plates, and the previously obtained equation (21) varies from 3.1% (R) to 7.2% (L). This small divergence demonstrates the reliability of the results obtained using the balance method and in the subsequent experiments.

Because of its good compatibility (1.8%) and reproducibility of its results, the total average Nusselt-Rayleigh relation obtained for the two vertical plates (20) has been taken as a reference for the balance method results obtained for the channels. This comparison shows that the convective convectioal heat transfer within the channels $s = 0.045 \text{ m}$ and $s = 0.18 \text{ m}$ is comparable to that obtained with the separate vertical plates and that the differences – +1.02% for $s = 0.045 \text{ m}$, -1.23% for $s = 0.085$ and +2.2 % for $s = 0.18 \text{ m}$ – are within the range of error.

Above results clearly show that the balance method is not precisely enough to perform a more detailed study of free convective heat transfer mechanisms in the channels, neither

does it allow the local nature of the phenomenon to be examined. Therefore, it was decided to continue further studies with the use of gradient method.

3.3. Results of gradient method investigations

Assuming that heat transfer from the isothermal vertical flat surfaces into the air inside the channel is two-dimensional, the local heat fluxes in a steady state at level y , described by Fourier's and Newton's relationships, should be the same, and can be written as:

$$-\lambda \cdot A \cdot \frac{\partial t}{\partial x} \Big|_{x=0,y} = \alpha_y \cdot A \cdot (t_w - t_{\infty,y}) \text{ and then } \alpha_y = \lambda \cdot \frac{\frac{\partial t}{\partial x} \Big|_{x=0,y}}{t_w - t_{\infty,y}}, \quad (22)$$

where t_w and $t_{\infty,y}$ °C are, respectively, the wall temperature and the lowest air temperature inside the channel at level y , α , W/(m²K) is the heat transfer coefficient and λ , W/(m·K) is the thermal conductivity of air.

The distributions of the local heat transfer coefficients $\alpha_{y,L}$ and $\alpha_{y,R}$, calculated using equation (22), from both vertical heated surfaces (L) and (R), as a function of temperature t_w and level y , for the three different channels ($s = 0.045$; 0.085 and 0.180) and two vertical heating plates ($s = \infty$), are given in Fig.8 The average values of the heat transfer coefficients for the left- and right-hand heated surfaces, determined from (23) and for the whole channels (24), are shown in the frames in Fig.8.

$$\overline{\alpha_{L/R}} = \frac{1}{H} \int_0^H \alpha_{y,L/R} dy = \frac{\lambda}{H} \int_0^H \frac{\frac{\partial t}{\partial x} \Big|_{x=0,y}}{t_w - t_{\infty,y}} dy, \quad (23)$$

$$\alpha = \frac{\overline{\alpha_L} + \overline{\alpha_R}}{2}. \quad (24)$$

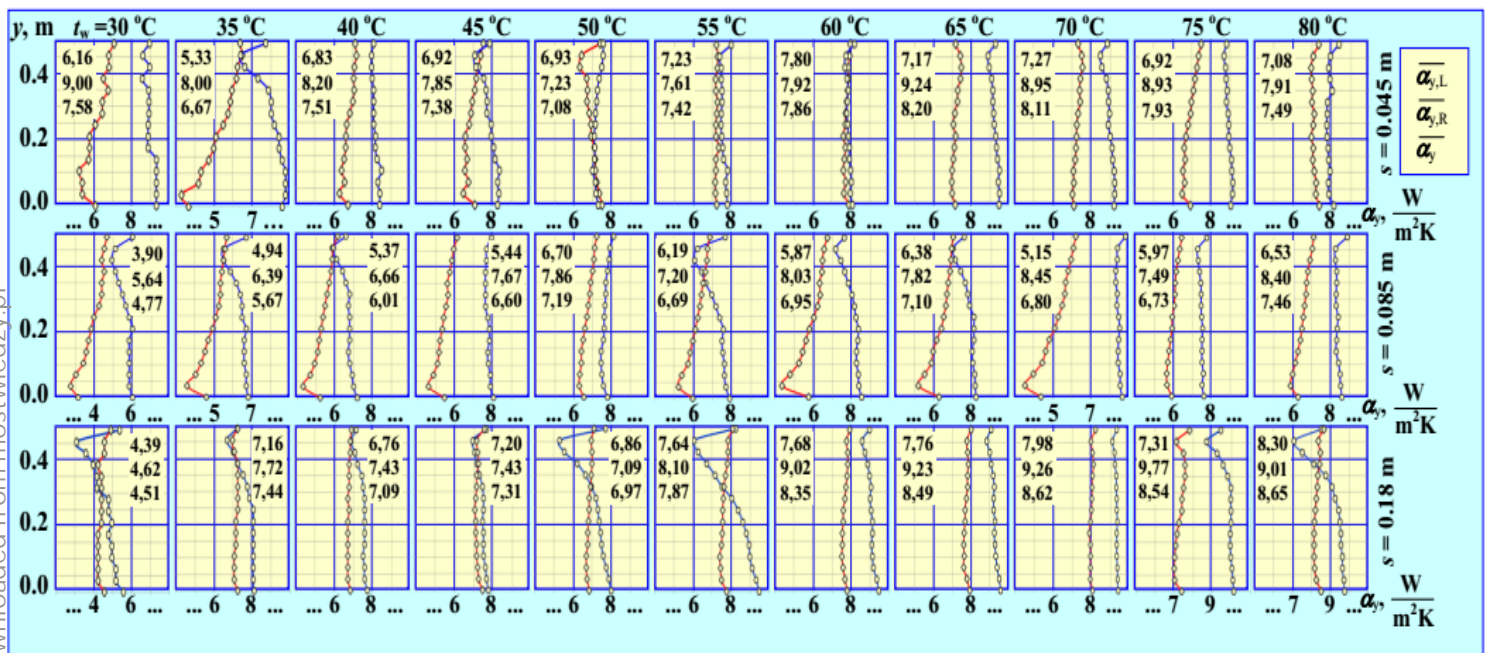


Fig.8 Distributions of local $\alpha_{y,L/R}$, average $\alpha_{L/R}$ and total α heat transfer coefficients on two (left – red diamonds, and right – blue circles) heated surfaces, which form gaps $s = 0.045$, 0.085 and 0.18 m at the channel half-width $z = B/2$, as a function of the temperature t_w of both heated surfaces.

Considering the influence of the variable properties of the surrounding air on the heat flow, the Nusselt Nu and Rayleigh Ra numbers for natural convection in the channels were defined as:

$$Nu = \frac{\alpha \cdot H}{\lambda} \quad \text{and} \quad Ra = \frac{g \cdot \beta \cdot (t_w - t_{\infty}) H^3}{\alpha \cdot \nu}, \quad (25)$$

where H , m – height of the heated plates (the characteristic linear dimension), g , m/s² – acceleration due to gravity, β , 1/K – **expansivity** coefficient of **cubic expansion** and a , ν , m²/s – thermal diffusivity and kinematic viscosity (see eq.17-20).

All the physical properties of the air a , β , ν and λ were specified for the average air temperature t_{av} . The investigation was carried out in an insulated room in order to prevent accidental air movements due to ventilation and draughts. For the surface temperature of both plates t_{wL} and t_{wR} , measured by thermocouples and the lowest air temperature in the channel at level y $t_{\infty,y}$ the average air temperature was determined as $t_{av} = (t_{wL} + t_{wR} + 2t_{\infty,y})/4$. In the case of the two vertical heated plates, which, because of the large distance $s = \infty$ between them did not influence each other, the surface temperature was additionally measured with the IR camera. If $t_{wL}=t_{wR}$ and $t_{\infty L}=t_{\infty R}$ the average air temperature t_{av} can be traditionally determined as $t_{av} = (t_{wL} + t_{wR})/2$.

The results of convective heat transfer for the channels, calculated using equation (25) in the form of the average Nusselt and Rayleigh numbers can be written as:

$$Nu = 1.094 \cdot Ra^{1/4}, \quad s = 0.045 \text{ m}, \quad (26)$$

$$Nu = 0.945 \cdot Ra^{1/4}, \quad s = 0.085 \text{ m}, \quad (27)$$

$$Nu = 1.073 \cdot Ra^{1/4}, \quad s = 0.180 \text{ m}, \quad (28)$$

Divergences between (17)-(19) and (26)-(28) are due to differences in the definition of Nusselt numbers Nub and Nu . In the case of balance method averaging of local values does not occurs, while in the gradient method it was necessary to perform.

In the gradient method the convective heat transfer from two vertical plates was investigated for seven wall temperatures – $t_w = 40; 45; 50; 55; 60; 65$ and 70 °C – with the local heat transfer coefficients being averaged independently for each plate α_{yL} and α_{yR} , in accordance with the procedures in (23) and (24). For sixteen temperatures t_w and moreover, instead of α_y , local Nusselt numbers Nu_y were averaged according to the formula:

$$Nu = \frac{1}{H} \int_0^H Nu_y dy = \frac{1}{H} \int_0^H \frac{\alpha_y}{\lambda} \cdot y \cdot dy = \frac{1}{H} \int_0^H \frac{-\frac{\partial t}{\partial x}|_{x=0,y}}{t_w - t_{\infty}} \cdot y \cdot dy. \quad (29)$$

Despite of the quantitative discrepancies the gradient method using the IR camera is practically more useful for qualitative investigations of heat transfer in channels than the balance one.

The results (26)-(28) shows that the **convective heat transfer intensity** **intensity of natural convective heat transfer** is the function of distance between plates s . The divergences are more visible in comparison with (17)-(19). The results with respect to the $s = 0.085$ with minimal effect, are the following: 15.8% for $s = 0.045$ m and 13.5% for $s = 0.180$ m.

The results obtained for the channels based on a characteristic linear dimension other than the height H , i.e. the distance between the plates s , were also calculated. The result, which is the relation $Nu^* = f(Ra^*)$ presented in the graph of Fig.9 can be written as:

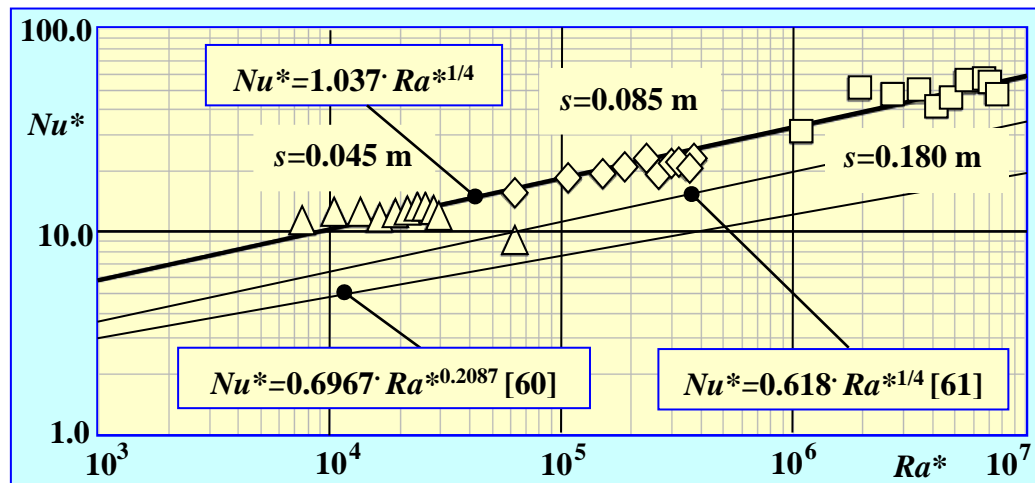
$$Nu^* = 1.037 \cdot Ra^{*1/4}. \quad (30)$$

where the Nusselt and Rayleigh numbers, modified for the channels, are defined as:

$$Nu^* = \frac{\alpha \cdot s}{\lambda} \quad \text{and} \quad Ra^* = \frac{g \cdot \beta \cdot (t_w - t_{\infty}) s^3}{a \cdot \nu} \frac{s}{H}, \quad (31)$$

It should be borne in mind that these results are one-dimensional, because they were obtained in the vertical planes in the centre of the space between the plates $z = B/2$ and perpendicular to their heated walls. A generalisation of these results is all the more true if $B/H \geq 1$.

Fig.9 shows the comparison of obtained results and the literature data presented by Fossa [60] and Rohsenow [61]. Visible discrepancies are caused by differences, in the case of paper [60] investigated channels were asymmetrically heated, while the correlation proposed by Rohsenow is the compilation of results of Churchill [45], Aung [17] and Elenbaas [21].



0

Fig.

9 Convective heat transfer in open channels as a function of distance between isothermal vertical heated surfaces s shown in the form of modified Nusselt-Rayleigh relations.

3.4. Mechanism of convective heat transfer inside the channels.

Analysis of the results, especially the visual ones, allows the structure of the convective flows of air inside the channels to be specified. Among these structures, one can specify four characteristic situations of overall natural convection heat transfer from the two vertical parallel isothermal plates forming the channel with an open circuit. Two of them are borderline and the other two intermediate:

- a – the first borderline case, when the spacing between the plates s is very close and much smaller than the height H or width B of the plates ($s_a \ll H$ and $s_a \ll B$): a fully developed flow pattern inside the channel is observed, which should, and as shown by further research, does indeed intensify heat transfer from the heated walls into the air.
- b – the second extreme situation occurs when the space between the plates is large $s_b \gg H$. Then, each plate transfers heat to air independently of the other – there is no interaction between the two plates either thermally or hydrodynamically. This case should be treated as the well-known problem of natural convective heat transfer from a single vertical plate.

It was observed that in the other two models the mechanism of convective heat transfer inside the channels is intermediate between the two extreme cases a) and b). Thermally developing regions also exist in both but in different forms:

- c – in the model with the plates also close together ($s_c \ll H$), but with the distance between the heating walls slightly larger than in the case of a) ($s_a < s_c$). This increase of s caused a partial inhibition of heat transfer.
- d – a further increase in the distance between the plates $s_d > s_c$, the thermal and flow activities of the two plates continue to interact with each other and likewise, the temperature profile along the channel continues to develop. However, with limited wall friction and air flow retardation inside the channel, the chimney effect intensifies, which in turn, as in the first extreme case, intensifies convective heat transfer.

4. Conclusions

This paper analyses natural convective heat transfer in air gaps between two vertical, parallel, isothermal and symmetrically heated plates, investigated using infrared techniques and the gradient method. It was demonstrated that this method is also applicable to investigations of more complex cases of convective heat transfer than those described in [57].

The sequentially presented results (temperature fields $t(x,y)$, temperature gradients distributions $\partial t / \partial x|_{x=0,y}$, distributions of heat transfer coefficients $\alpha(x,y)$ and averaged Nusselt numbers $Nu(Ra)$) show their logical correctness and consistency. Consequently, they can provide a basis for describing and interpreting the convective heat transfer phenomenon examined in this work.

This study confirmed that there is a simple correlation between the width of the gap between heated walls s on the intensity of convective heat transfer in open channels (30). The results demonstrated the inhibition or intensification of heat transfer in accordance with s . We hope that other researchers may find this method useful for practical application in the structural design and construction of air heat exchangers, radiators or coolers.

Acknowledgement - This work was supported by the National Science Centre, Poland, UMO-2015/17/N/ST8/02716.

References:

- [1] A-J.N. Khalifa, Natural convective heat transfer coefficient - a review II. Surfaces in two- and three-dimensional enclosures, *Energy Conversion and Management*, 42 (2001) 505-517.
- [2] A. Baïri, E. Zarco-Pernia, J.M. García de María, A review on natural convection in enclosures for engineering applications. The particular case of the parallelogrammic diode cavity, *Applied Thermal Engineering*, 63 (2014) 304-322.
- [3] M. Nansteel, R. Greif, Natural convection in undivided and partially divided rectangular enclosures, *Journal of Heat Transfer*, 103 (1981) 623-629.
- [4] J.K. Platten, J.C. Legros, *Convection in Liquids*, part.C, Springer-Verlag, 1983.
- [5] H.K. Wee, *Heat and Mass Transfer in confined spaces*, PhD thesis, University of Canterbury, 1986.
- [6] F. Penot, A. Ndam, Successive bifurcations of natural convection in vertical enclosure heated from the side, *1st European Thermal Sciences*, vol. 1, Birmingham, UK, 1992, pp. 507-514.
- [7] A. Baïri, N. Laraqi, J.M. García de María, Numerical and experimental study of natural convection in tilted parallelepipedic cavities for large Rayleigh numbers, *Experimental Thermal and Fluid Science*, 31 (2007) 309-324.
- [8] E.M. Sparrow, P.A. Bahrami, Experiments on Natural Convection from Vertical Parallel Plates with Either Open or Closed Edges, *J. Heat Transfer*, 102(2) (1980) 221-227.
- [9] G. Desrayaud, E. Chenier et al., Benchmark solutions for natural convection flows in vertical channels submitted to different open boundary conditions, *International Journal of Thermal Sciences*, Elsevier, 72 (2013) 18-33.
- [10] P. Kiš, H. Herwig, Natural convection in a vertical plane channel: DNS results for high Grashof numbers, *Heat Mass Transfer*, Springer-Verlag Berlin Heidelberg 50(7) (2014) 957-972. DOI 10.1007/s00231-014-1305-5.
- [11] A.G. Fedorov, R. Viskanta, Turbulent natural convection heat transfer in an asymmetrically heated, vertical parallel-plate channel, *International Journal of Heat Mass Transfer*, 40 (16) (1997) 3849-3860.
- [12] M.A. Habib, S.A.M. Said, S.A. Ahmed, A. Asghar, Velocity characteristics of turbulent natural convection in symmetrically and asymmetrically heated vertical channels, *Experimental Thermal and Fluid Science*, 26 (2002) 77-87.
- [13] F.J. Higuera, Yu.S. Ryazantsev, Natural convection flow due to a heat source in a vertical channel, *International Journal of Heat and Mass Transfer*, 45 (2002) 2207-2212.
- [14] T.Yilmaz, S.M.Fraser, Turbulent natural convection in a vertical parallel-plate channel with asymmetric heating, *International Journal of Heat and Mass Transfer*, 50 (2007) 2612-2623.
- [15] W.H. McAdams, *Heat Transmission*, McGraw Hill, New York, 1954.
- [16] E.M. Sparrow, L.F.A. Azevedo, Vertical channel natural convection spanning between the fully developed limit and single plate boundary layer limit, *International Journal of Heat and Mass Transfer*, 28 (1985) 1847-1857.
- [17] W. Aung, L.S. Fletcher, V. Sernas, Developing laminar free convection between vertical plates and asymmetric heating, *International Journal of Heat and Mass Transfer*, 16 (1972) 2293-2308.
- [18] A.L. Pica, G. Rodno, R. Volpes, An experimental investigation on natural convection of air in a vertical channel, *International Journal of Heat and Mass Transfer*, 50 (2007) 2612-2623.

- [19] A. Andreozzi, B. Buonomo, O. Manca, Transient Natural Convection in Vertical Channels Symmetrically Heated at Uniform Heat Flux, *Numerical Heat Transfer, Part A: Applications: An International Journal of Computation and Methodology*, 55 (2009) 409-431.
- [20] Z. Amine, C. Daverat, S. Xin, S. Giroux-Julien, H. Pabiau, C. Ménézo, Natural Convection in a Vertical Open-Ended Channel: Comparison between Experimental and Numerical Results, *Journal of Energy and Power Engineering* 7 (2013) 1265-1276.
- [21] W. Elenbass, Heat dissipation of parallel plates by free convection, *Physica*, 9 (1942) 1–28.
- [22] G.D. Raithby, K.G.T. Holland, A general method of obtaining approximate solution to laminar and turbulent free convective problems. *Advanced Heat Transfer*, 11 (1975) 266-315.
- [23] G.D. Raithby, K.G.T. Holland, Natural convection, W.M. Rosenhow, J.P. Hartnett, E.N. Ganic (Eds.), *Handbook of Heat Transfer Fundamentals* (second ed.), McGraw-Hill, New York (1985) (Chapter 6)
- [24] S.J. Ormiston, A numerical study of two-dimensional natural convection in a Trombe wall system including vent and room effects. M.A.Sc. Thesis, Dept. of Mechanical Engineering, University of Waterloo (December 1983).
- [25] L. Martin, G.D. Raithby, M.M. Yovanovich, On the Law Rayleigh Number Asymptote for Natural Convection Through an Isothermal, Parallel-Plate Channel, *ASME Journal of Heat Transfer*, 113 (1991) 899-905.
- [26] H.M. Salih, Numerical Simulation for Laminar Natural Convection with in a Vertical Heated Channel, *Eng. & Tech. Journal*, 29(11) (2011), 2298-2311.
- [27] J.R. Bodia, J.F. Osteral, The development of free convection between heated vertical plates *ASME J. Heat Transfer*, 84 (1962) 40–44.
- [28]. N.A.A.Qasem, B.Imtryaz, R.Ben-Mansour, M.A.Habib, Effect of Radiation Heat Transfer on Naturally Driven Flow Through Parallel-Plate Vertical Channel, *Arab. J. Sci. Eng.*, Published online 17 October 2016, DOI 10.1007/s13369-016-2319-8.
- [29] A.L. Pica, G. Rodono, R. Volpes, An experimental investigation of free convection heat transfer in vertical channels with backward facing step, *ASME, Fluids Eng.Div.* 238 (3) (1993) 263–270.
- [30] A. Daloglu, T. Ayhan, Natural convection in a periodically finned vertical channel, *Int. Commun. Heat Mass Transfer* 26 (8) (1999) 1175–1182.
- [31] S.C. Lin, K.P. Chang, Y.H. Hung, Natural convection within a vertical finite-length channel in free space, *J. Thermophys. Heat Transfer* 8 (2) (1994) 366–368.
- [32] T. Inagaki, K. Komori, Numerical modeling on turbulent transport with combined forced and natural convection between two vertical parallel plates, *Int. J. Comput. Meth. A* 27 (4) (1995) 417–431.
- [33] A.K. Singh and T. Paul, Transient natural convection between two vertical walls Heated/Cooling Asymmetrically, *International Journal of Applied Mechanics and Engineering*, 11(1) (2006) 143-154.
- [34] G. Tanda, Natural convective heat transfer in vertical channels with low-thermal conductivity ribs, *International Journal of Heat and Fluid Flow*, 29 (2008) 1319–1325.
- [35] D. Ospir, C. Chereches, C. Popa, S. Fohanno, C. Popovici, Flow dynamics in a double-skin façade, *Proceedings of the 3rd WSEAS International Conference on Finite Differences – Finite Elements – Finite Volumes – Boundary Elements* (2009).
- [36] A. Mokni, H. Mhiri, G. Le Palec, Ph. Bournot, Mixed convection in a vertical heated channel: influence of the aspect ratio, *International Journal of Engineering and Applied Sciences* 5(1) (2009) 60-66.
- [37] K.M. Çakar, Numerical investigation of natural convection from vertical plate finned heat sinks, M.Sc. Thesis submitted to The Middle East Technical University (2009).
- [38] N. Srivastava, A.K. Singh, Mixed convection in a composite system bounded by vertical walls, *Journal of Applied Fluid Mechanics*, 3(2) (2010) 65-75.
- [39] Q. Lu, S. Qiu, G. Su., W. Tian, Z. Ye, Experimental research on heat transfer of natural convection in vertical rectangular channels with large aspect ratio, *Experimental Thermal and Fluid Science* 34 (2010) 73–80.
- [40] A. Bar-Cohen, W.M. Rohsenow, Thermally Optimum Spacing of Vertical, Natural Convection Cooled, Parallel Plates, *ASME Journal of Heat Transfer*, 106(1) (1984) 116-124.
- [41] A. Bar-Cohen, H. Schweitzer, Convective immersion cooling of parallel vertical plates. *Hybrids, and Manufacturing Technology*, *IEEE Transactions* 8(3) (1985) 343-351.
- [42] J.L. Wright H. Jin, K.G.T. Hollands, D. Naylor, Flow visualization of natural convection in a tall, air-filled vertical cavity, *International Journal of Heat and Mass Transfer* 49(5) (2006) 889-904.



- [43] Z.Y. Guo, Y.Z. Song, X.W. Zhao, Experimental Investigation on Natural Convection in Channel by Laser Speckle Photography, *Experimental Thermal and Fluid Science*, 4 (1991) 594-600.
- [44] K. Kato et al. Heat Transfer in a Channel between Vertical Electronic Circuit Boards Cooled by Natural Air Convection, *Journal of Chemical Engineering of Japan* 24(5) (1991) 568-574.
- [45] S.W. Churchill, R. Usagi, A General Expression for the Correlation of Rates of Transfer and Other Phenomena, *AIChE Journal*, 18(6) (1972) 1121-1128.
- [46] O. Miyatake, T. Fujii, M. Fujii, H. Tanaka, Natural Convective Heat Transfer Between Vertical Parallel Plates – One Plate with a Uniform Heat Flux and the other Thermally Insulated, *Heat Transfer – Japanese Research*, 4 (1973) 25-33.
- [47] O. Miyatake, T. Fujii, Free Convective Heat Transfer Between Vertical Plates – One Plate Isothermally Heated and the Other Thermally Insulated, *Heat Transfer – Japanese Research*, 3 (1972) 30-38.
- [48] S. Taieb, L.A. Hatem, J. Balti, Natural convection in an asymmetrically heated vertical channel with an adiabatic auxiliary plate, *International Journal of Thermal Sciences*, 74 (2013) 24-36.
- [49] E.R.G. Eckert, W.O. Carlson, Natural Convection in an Air Layer Enclosed Between Two Vertical Plates with Different Temperatures, *International Journal of Heat and Mass Transfer*, 2 (1961) 106-120.
- [50] V.I. Terekhov, A.L. Ekaid, Laminar Natural Convection between Vertical Isothermal Heated Plates with Different Temperatures, *Journal of Engineering Thermophysics*, 20(4) (2011) 416–433.
- [51] T. Inagaki, S. Maruyama, Turbulent Heat Transfer of Natural Convection Between Two Vertical Parallel Plates, *Heat Transfer – Asian Research*, 31(1) (2002) 56-67.
- [52] A.S. Krishnan, B. Premachandran, C. Balaji, S.P. Venkateshan, Combined experimental and numerical approaches to multi-mode heat transfer between vertical parallel plates, *Experimental Thermal and Fluid Science*, 29 (2004) 75–86.
- [53] T. Yilmaz, S.M. Fraser, Turbulent natural convection in a vertical parallel-plate channel with asymmetric heating, *International Journal of Heat and Mass Transfer* 50 (2007) 2612–2623.
- [54] R.A. Writz, R.J. Stulzman, Experiments on Free Convection Between Vertical Plates With Symmetric Heating, *International Journal of Heat Transfer*, 104 (1982) 501-507.
- [55] G. Polidori, S. Fatnassi, R. Ben Maad, F. Beaumont, S. Fohanno, Transient natural convection flow dynamics in a asymmetrically heated vertical channel, 10th International Conference on Heat Transfer, Fluid Mechanics and Thermodynamics 14–16 July 2014.
- [56] D. Ambrosini, D. Paoletti, G. Tanda, Investigation of natural convection in channels by optical techniques, Conference: XX Congresso UIT, At Maratea (Italy), June 2002, p.1-6.
- [57] W.M. Lewandowski, M. Ryms, H. Denda, E. Klugmann-Radziemska, Possibility of thermal imaging use in studies of natural convection heat transfer on the example of an isothermal vertical plate, *International Journal of Heat and Mass Transfer*, 78 (2014) 1232-1242.
- [58] B. Rama Bhupal Reddy, A numerical study on developed laminar mixed convection with vertical channel in downflow, *International Journal of Physical and Social Sciences*, 2(3) (2012) 72-88.
- [59] W.Aung, G. Worku, Developing flow and flow reversal in a vertical channel with asymmetric wall temperatures, *ASME Journal of Heat Transfer* 108 (1986) 299–304.
- [60] M.Fossa, C.Menezo, E.Leonardi, Experimental natural convection on vertical surfaces for building integrated photovoltaic (BIPV) applications, *Experimental Thermal and Fluid Science* 32 (2008) 980–990.
- [61] W.M.Rohsenow, J.P.Hartnett, Y.I.Cho, *Handbook of Heat Transfer*, McGraw-Hill, New York, 1998.

Nomenclature

- a*** - thermal diffusivity, m²/s
- b*** - half-width of channel, $\equiv s/2$, m
- A*** - area, $\equiv 2HB$, m²; coefficient
- B*** - plate width, m
- C*** - coefficient
- g*** - acceleration due to gravity, m/s²
- H*** - channel or vertical plate length, m
- I*** - amperage of electric current, A

m - exponent in Eqs. (2) and (5)
 Nu_b - channel balance Nusselt number, $\equiv UI/(\lambda(t_w - t_\infty)B)$ dimensionless
 \widetilde{Nu} - modified Nusselt number, $\equiv UIs/(\lambda(t_w - t_\infty)H^2)$ dimensionless
 Nu_y - local Nusselt number, $\equiv \alpha y/\lambda$ dimensionless
 Nu - total Nusselt number, Eq. (25), dimensionless
 Nu^* - total channel Nusselt number, $\equiv \alpha s/\lambda$, dimensionless
 P - plate/air parameter in Eq. (22), $\equiv Ra/H^4$, m^{-4}
 q'' - heat flux, $\equiv q/A$, W/m^2
 Ra_b - Rayleigh number, $\equiv g\beta\Delta t H^3/(\nu\alpha)$, dimensionless
 Ra^* - channel Rayleigh number, $\equiv g\beta\Delta t s^3/(\nu\alpha)s/H$, dimensionless
 \widetilde{Ra} - modified Rayleigh number, $\equiv g\beta\Delta t b^3/(\nu\alpha)H/b$, dimensionless
 s - plate spacing, m
 t - temperature, $^{\circ}C$
 U - voltage of electric current, V
 x, y, z - coordinates, m

Greek Letters

α - heat transfer coefficient, Eq. (13) $W/(m^2 K)$
 β - volumetric coefficient of thermal expansion, $1/K$
 λ - thermal conductivity, $W/(m K)$
 ν - kinematic viscosity, m^2/s
 ρ - density, kg/m^3
 ∞ - entrance or ambient value

Subscripts

a - auxiliary
 av - average,
 b - balance method
 L - left,
 m - main,
 R - right,
 w - wall,
 y - local